

Co-optimization of power line shutoff and restoration for electric grids under high wildfire ignition risk

Noah Rhodes and Line Roald

Abstract—Electric power infrastructure has ignited several of the most destructive wildfires in recent history. Preemptive power shut-offs are an effective tool to mitigate the risk of ignitions from power lines, but at the same time can cause widespread power outages. Electric utilities are thus faced with the challenging trade-off of where and when to implement these shut-offs, as well as how to most efficiently restore power once the wildfire risk is reduced. This work proposes a mathematical optimization problem to help utilities make these decisions. Our model co-optimizes the power shut-off (considering both wildfire risk reduction and power outages) as well as the post-event inspection and energization of lines. It is implemented as a rolling horizon optimization problem that is resolved whenever new forecasts of load and wildfire risk become available. We demonstrate our method on the IEEE RTS-GMLC test case using real wildfire risk data US Geological Survey, and investigate the sensitivity of the results to the forecast quality, decision horizon and system restoration budget. The software implementation is available in the open source software package *PowerModelsWildfire.jl*.

I. INTRODUCTION

Wildfire ignitions caused by electrical equipment are an increasing concern for power grid operators. A study of Australia’s bushfires found that electrical infrastructure accounts for 30% of ignitions during droughts and heat-waves [1]. In California, the state firefighting organization’s annual wildfire activity report *Redbook* reports that between 2015-2020, the 10% of wildfires that were ignited by electrical equipment were responsible for more than 70% of damages (\$17.5 billion) [2].

Research on interactions between wildfires and the electric grid *after* a fire has been ignited include derating of power line capacity near a progressing wildfire [3], [4] and fast simulations of wildfire spread to provide early warnings for transmission line shutdowns [5]. However, the focus has recently shifted towards how to reduce the risk of wildfire ignitions. Refs. [6]–[9] review approaches to reduce the risk of ignitions, and adaptations of this kind are already being planned by utilities. For example, Pacific Gas & Electric (PG&E) announced an initiative to underground 10,000 miles of distribution lines over the course of more than a decade at a cost of \$20 billion [10], along with other measures such as more frequent vegetation clearing within the right of way of power lines. Unfortunately, the significant cost and need for qualified crews and equipment means that these risk reduction approaches take time to implement.

This work was supported by the U.S. National Science Foundation ASCENT program under award 2132904. N. Rhodes and L. Roald are with the Department of Electrical and Computer Engineering, University of Wisconsin-Madison, USA. Email: {nrhodes, roald}@wisc.edu

Meanwhile, power system operators rely on short-term measures to reduce risk, including changes to the protection system settings (i.e. disabling of automatic reclosing) [3] or Public Safety Power Shutoffs (PSPS), which de-energize grid equipment during high wildfire risk events. While highly effective in reducing wildfire risk [11], PSPS leads to intentional disconnection of customers, causing large scale power outages that may last for days [12]. Since the economic and health impacts of power outages can be significant, it is important to balance the benefits of wildfire risk reduction with the impacts of power outages. To this end, [13] proposed a framework to optimally balance wildfire risk reduction and power outage sizes when deciding which lines to shut off. Other approaches include data-driven methods to plan PSPS by training machine learning models with optimization problems results [14], [15], or using a dynamic programming approach to optimize a PSPS [16]. These methods focus on accelerating the solution time of a planned PSPS for improved use on large networks in real time. Ref. [17] proposes an optimal investment model that considers installation of batteries and under-grounding power lines to mitigate and reduce the impact of PSPS.

Although the above methods may be effective in identifying locations where the implementation of PSPS is required, they do not explicitly consider how to effectively restore the system once the wildfire risk is reduced. A main reason for the prolonged outages following a PSPS event is that utility crews must manually inspect the de-energized power lines for damage that could cause ignitions before they can be placed back into operation. Thus, while de-energization of a line can happen instantaneously, the re-energization (or restoration) can take hours or days [18]. To make optimal decisions about which lines to de-energize, it is therefore necessary to assess how de-energization impacts the risk of wildfire ignitions and power outages both during the initial shut-down and throughout the restoration process.

To address this question, we develop a *multi-period optimal power shut-off* (MOPS) problem to co-optimize power line shut-offs and restoration for the power grid in situations with high wildfire risk. The formulation combines and extends our prior work on balancing wildfire risk and power outages for a single time period [13] and post-disaster restoration planning [19]. The objective function maximizes the electric load served to customers, while minimizing total wildfire risk, and accounting for utility capacity to perform line inspections.

Since the optimal operational decisions depend on the current and forecasted risk and must be updated as new

information becomes available (e.g. every day), we formulate the problem as a *rolling horizon* optimization problem. The problem is challenging to solve due to the presence of binary variables representing the on/off status of the transmission lines, as well as the large number of grid constraints across multiple time periods [19]. In our case study, we therefore investigate the impact of the decision horizon on the solution quality. We also assess how forecast errors for the wildfire risk and different restoration budgets impact the solution.

In summary, the contributions of this paper are 1) a rolling horizon, multi-period optimization model which co-optimizes public safety power shutoffs and the subsequent grid restoration, 2) analysis of the sensitivity of the problem to several parameters including the forecast errors, forecast horizon and the restoration budget.

The remainder of the paper is organized as follows. Section II introduces the problem formulation. Section III presents the case study and problem setup, and analysis of the results. Section IV concludes the work.

II. MODELING AND PROBLEM FORMULATION

In this section, we formulate the Multi-period Optimal Power Shutoff (MOPS) problem. MOPS is a rolling horizon optimization model that provides an optimized schedule for both power line shut-offs and restoration, and combines and extends the single-period optimal power shut-off model in [13] and the grid restoration planning model in [19].

A. Rolling Horizon Formulation

We envision a grid operator of a power grid with a set of nodes \mathcal{N} , lines \mathcal{L} , generators \mathcal{G} and loads \mathcal{D} . This grid has elevated wildfire risk, and the operator is considering a public safety power shutoff to mitigate the wildfire threat. The operator must make decisions on the power lines they may shutdown, customers they may disconnect, and how to bring the grid back online in the future. Their goal is to reduce wildfire risk while minimizing customer power outages and maintaining grid reliability.

Wildfire risk depends on ambient conditions such as vegetation cover, humidity and wind speed, and is updated on a regular basis. For example, the Wildland Fire Potential Index (WFPI) [20] is released daily and provides both current and 7-day forecasts for the contiguous United States. Due to the evolving nature of these forecasts, it makes sense to (i) take the forecasts into account when deciding on an optimal schedule for public safety power shut-offs and restoration, and (ii) update the schedule daily as new information becomes available. We therefore formulate our problem as a rolling horizon optimization problem with forecast horizon \mathbf{H} , as shown in Model 1 (and further explained below). Each day T , a Multi-period Optimal Power Shutoff (MOPS) problem is solved for all timesteps $t \in \mathcal{T}$ where $\mathcal{T} = \{T, \dots, T + \mathbf{H}\}$. The power shut-off and restoration actions for the first day $t = T$ are then implemented on the power grid. The next day, we repeat the process, given the current status of the grid and updated forecast information.

B. Objective function

The system operator is pursuing three different objectives, namely maximizing load, minimizing wildfire risk and maintaining grid reliability. We first describe how these three objectives are evaluated.

1) *Load served*: The load D_{Served} is calculated as

$$D_{Served} = \sum_{t \in \mathcal{T}} \sum_{d \in \mathcal{D}} x_{dt} w_{dt} \mathbf{P}_{dt}^D. \quad (1)$$

Here, \mathbf{P}_{dt}^D is a parameter expressing the total demand for electricity from load d at time period t and w_{dt} is a weight used to express increased priority for certain load (e.g. a hospital may have a higher weight). We assume that load can be continuously shed, with the continuous decision variable x_{dt} representing the percentage of load that is served. The total demand served D_{Served} is obtained by summing over all loads $d \in \mathcal{D}$ and all time periods $t \in \mathcal{T}$.

2) *Wildfire risk*: We express the total risk of wildfire ignitions based on the wildfire risk associated with each transmission line in the network, i.e.

$$R_{Fire} = \sum_{t \in \mathcal{T}} \sum_{ij \in \mathcal{L}} z_{ijt} \mathbf{R}_{ijt} \quad (2)$$

Here, \mathbf{R}_{ijt} represents the risk of a wildfire ignition from line ij at time t if the line is energized (we discuss how to obtain these risk values in the case study). The binary decision variable z_{ijt} represents the status of the line, with $z_{ijt} = 1$ indicating that it is on and $z_{ijt} = 0$ indicating that it is off. By choosing to de-energize the line, i.e. setting $z_{ijt} = 0$, we can thus reduce the wildfire risk of line ij at time t to zero.

3) *Grid Vulnerability*: Because the grid benefits from having many transmission lines and multiple paths for power to flow along, we want to avoid disabling very low risk lines, even if they do not contribute to serving more power, because this reduces the redundancy in the transmission network. We also therefore include a penalty in the objective for each line that is disabled, expressed as grid vulnerability \mathbf{V} ,

$$V_{system} = \sum_{t \in \mathcal{T}} \sum_{ij \in \mathcal{L}} (1 - z_{ijt}) \mathbf{V} \quad (3)$$

Here, \mathbf{V} represents the vulnerability of turning an individual line off and V_{System} represents the total vulnerability of the network.

Given the above modeling considerations, we formulate the objective function (5a). In the objective, we include R_{Fire} and V_{System} in a single term and observe that $R_{Fire} - V_{System}$ is equivalent to

$$R_{Fire} - V_{System} = |\mathcal{L}| |\mathcal{T}| \mathbf{V} + \sum_{t \in \mathcal{T}} \sum_{ij \in \mathcal{L}} z_{ijt} (\mathbf{R}_{ijt} - \mathbf{V})$$

The second term in this expression highlights that \mathbf{V} represents the minimum wildfire risk for which it is beneficial to disable a line. Choosing a non-zero value for \mathbf{V} thus provides an incentive to keep low risk lines, or lines that may be low risk in the future, energized to increase redundancy.

The objective function (5a) uses the total load D_{Tot} and the total wildfire risk R_{Tot} before a power shut-off as normalization factors, with D_{Tot} , R_{Tot} defined as

$$D_{Tot} = \sum_{t \in \mathcal{T}} \sum_{d \in \mathcal{D}} P_{dt}^D, \quad R_{Tot} = \sum_{t \in \mathcal{T}} \sum_{ij \in \mathcal{L}} R_{ijt}$$

This normalization implies that the objective functions expresses the percentage of load or wildfire risk after implementation of the PSPS, with $0 \leq D_{Served}/D_{Tot} \leq 1$ and $0 \leq R_{Fire}/R_{Tot} \leq 1$.

Finally, the value $\alpha \in [0, 1]$ allows us to express a preference for either focusing on serving load or mitigating wildfire risk. The preference for mitigating wildfire risk vs limiting grid vulnerability is expressed by our choice of the parameter V .

C. Restoration Constraints

An important aspect of our formulation is that the utility has a limited budget to inspect and restore power lines after a public safety power shut-off. The limits on how much restoration can happen in each time period is described by constraints (5e)-(5g). Constraint (5f) sets the indicator variable for restoration y_{ijt}^L to 1 if a line is off in the previous period $z_{ijt-1}^L = 0$ and on in the current period $z_{ijt}^L = 1$. These logical constraints are implemented in the optimization problem by (4), where the three inequalities form the logical *and* operation, and the *negation* of z_{ijt-1}^L by subtracting the variable from the value 1.

$$y_{ijt}^L \leq (1 - z_{ijt-1}^L) \quad (4a)$$

$$y_{ijt}^L \leq z_{ijt}^L \quad (4b)$$

$$y_{ijt}^L \geq (1 - z_{ijt-1}^L) + z_{ijt}^L - 1 \quad (4c)$$

Constraint (5e) implements the same constraint for the initial condition z_{ij0}^L of the line in the first period. Constraint (5g) limits the amount of restoration that can occur in a single period according to the budget available Y_t . The cost of restoring a line scales with length ℓ_{ij} , because the primary action in restoring a line is to inspect the line for damage to ensure it will not cause a spark when it is energized. The parameter Y_t can thus be understood as the total length of line that the utility is able to inspect in time step t . Finally, (5h) enforces that z_{ijt}^L and y_{ijt}^L take on binary values.

D. Power Flow Constraints

To model how de-energization and restoration of lines impact the amount of electricity served to customers, it is important to model the power flows in the system. Equations (5i)-(5n) uses a DC power flow formulation to model the power flow in each time period, accounting for shedding load and de-energized/restored lines.

Nodal power balance is enforced by (5i) where total generation P_{gt}^G , transmission line power P_{ijt}^L , and load served $x_{dt}^D P_{dt}^D$ must sum to zero. Eq. (5j) ensures that the load shed proportion x_{dt}^D is constrained to be within 0 and 1. The constraint in (5k) constrains the power P_{gt}^G from each generator g to between 0 and its upper power limit \overline{P}_{gt}^G . The

Model 1 Multi-period Optimal Power Shutoff (MOPS)

variables: $(\forall t \in \mathcal{T})$

$$P_{gt}^G \forall g \in \mathcal{G}, \quad P_{ijt}^L \forall (i, j) \in \mathcal{L}, \quad \theta_{it} \forall i \in \mathcal{B}, \\ x_{dt}^D \forall d \in \mathcal{D}, \quad z_{ijt}^L \forall (i, j) \in \mathcal{L}, \quad y_{ijt}^L \forall (i, j) \in \mathcal{L}$$

$$\textbf{maximize:} (1 - \alpha) \frac{D_{Served}}{D_{Tot}} - \alpha \left(\frac{R_{Fire} - V_{System}}{R_{Tot}} \right) \quad (5a)$$

subject to $\forall t \in \mathcal{T}$:

$$D_{Served} = \sum_{t \in \mathcal{T}} \sum_{d \in \mathcal{D}} x_{dt} w_{dt} P_{dt}^D \quad (5b)$$

$$R_{Fire} = \sum_{t \in \mathcal{T}} \sum_{ij \in \mathcal{L}} z_{ijt} R_{ijt} \quad (5c)$$

$$V_{system} = \sum_{t \in \mathcal{T}} \sum_{ij \in \mathcal{L}} (1 - z_{ijt}) V \quad (5d)$$

$$y_{ij1}^L = (\neg z_{ij0}^L) \wedge z_{ij1}^L \quad \forall (i, j) \in \mathcal{L}, \text{ for } t = T \quad (5e)$$

$$y_{ijt}^L = (\neg z_{ijt-1}^L) \wedge z_{ijt}^L \quad \forall (i, j) \in \mathcal{L}, \text{ for } t \neq T \quad (5f)$$

$$\sum_{(ij) \in \mathcal{L}} y_{ijt}^L \ell_{ij} \leq Y_t \quad (5g)$$

$$z_{ijt}^L \in \{0, 1\}, \quad y_{ijt}^L \in \{0, 1\} \quad \forall (i, j) \in \mathcal{L} \quad (5h)$$

$$\sum_{g \in \mathcal{G}_i} P_{gt}^G + \sum_{(i,j) \in \mathcal{L}_i} P_{ijt}^L - \sum_{d \in \mathcal{D}_i} x_{dt}^D P_{dt}^D = 0 \quad \forall i \in \mathcal{B} \quad (5i)$$

$$0 \leq x_{dt}^D \leq 1 \quad \forall d \in \mathcal{D} \quad (5j)$$

$$0 \leq P_{gt}^G \leq \overline{P}_{gt}^G \quad \forall g \in \mathcal{G} \quad (5k)$$

$$-\overline{P}_{ij}^L z_{ijt}^L \leq P_{ijt}^L \leq \overline{P}_{ij}^L z_{ijt}^L \quad \forall (i, j) \in \mathcal{L} \quad (5l)$$

$$P_{ijt}^L \leq -b_{ij}(\theta_{it} - \theta_{jt}) + \overline{\theta}_{ij}^{\Delta}(1 - z_{ijt}^L) \quad \forall (i, j) \in \mathcal{L} \quad (5m)$$

$$P_{ijt}^L \geq -b_{ij}(\theta_{it} - \theta_{jt}) + \underline{\theta}_{ij}^{\Delta}(1 - z_{ijt}^L) \quad \forall (i, j) \in \mathcal{L} \quad (5n)$$

upper limit may vary with the time period t for renewable energy sources, based on the forecasted maximum output. While this problem formulation can support non-zero lower bounds on generation, we remove the unit commitment aspect for simplicity.

Equation (5l) constrains the power flow P_{ijt}^L on the line from i to j between the power limits $-\overline{P}_{ij}^L z_{ijt}^L$ and $\overline{P}_{ij}^L z_{ijt}^L$ when the line is active and $z_{ijt}^L = 1$. When a line is inactive, $z_{ijt}^L = 0$, the power flow across the line is 0. Equations (5m) and (5n) define the relationship between voltage angle differences and line power flow, while accounting for when a line becomes disabled. When a line is active, $z_{ijt}^L = 1$, these constraints reduce to ordinary linearized DC power flow,

$$P_{ijt}^L = -b_{ij}(\theta_{it} - \theta_{jt}), \quad (6)$$

where b_{ij} is the line susceptance, and θ_{it} and θ_{jt} are the bus voltage angles for bus i and j at time t . When the line is inactive, $z_{ijt} = 0$, the power flow is decoupled from the voltage angle difference through the big-M values $\overline{\theta}_{ij}^{\Delta}$ and $\underline{\theta}_{ij}^{\Delta}$, which can be calculated as in [21]. This allows the power flow to be constrained to 0 in (5l) without constraining the voltage angle differences.

III. CASE STUDY

We demonstrate the use of our proposed model and study the sensitivity to the forecast horizon, restoration budget and

the vulnerability penalty of disabling lines.

A. Case study setup

We first describe our implementation and the data used to set up our case study.

1) *Implementation*: The optimization model is available in the open source package *PowerModelsWildfire.jl* [13], implemented in the Julia language [22], and solved using the Gurobi v9.1 optimization solver [23].

2) *Test System*: We base our case study on the RTS-GMLC [24] system. This synthetic test system has geographic coordinates located in southern California, a region which has been affected by Public Safety Power Shut-Offs. There are one year of hourly load and renewable energy profiles available for the system, and we choose to use data from the month of October. For each day, we pick the hour with the highest load forecast.

To obtain a case with an interesting level of congestion, we increased the active power demand using the API method in [25], which proportionally increases each load in the system until transmission line limits are constrained. This resulted in a 2.14x increase of load and generation in the network, and a higher utilization of the transmission network.

3) *Wildfire risk data*: Wildfire risk data was obtained from the United States Geological Survey's (USGS) Wildland Fire Potential Index (WFPI) [20] which estimates the potential a one-acre fire will spread and burn more than 500-acres. This measure incorporates fuel models and forecast information for precipitation, dry bulb temperature and wind speeds to create a daily forecast of the WFPI for up to 7 days. For each line and each day, we calculate the wildfire risk as the highest WFPI value along the line, in accordance with [26]. Using the maximum risk implies that we focus on minimizing risk at particularly risky locations.

To provide an overview of the wildfire risk data, Figure 1a shows a histogram of all the realized wildfire risk values (i.e. not including forecasted data) for all lines and all days in the month of October. We observe that many lines have either zero risk or risk in the range between 70-120. There is a small number of lines that have very high risk > 160 . Figure 1b shows the total system risk before any power shut-offs (i.e., the sum of all wildfire risk values for all lines, assuming all lines are energized) based on the forecasted (in red) and realized (in black) wildfire risk values. We observe that there are substantial forecast errors, with the forecast sometimes underestimating and sometimes overestimating the risk.

4) *Baseline Parameters*: For our case study, we set $\alpha = 0.7$ as we found this to provide a reasonable trade-off between load shed and risk. We further use the following default parameter selections, unless otherwise specified:

- *Optimality Gap*: 0.01%
- *Solver Time Limit*: 1 hour
- *Restoration Budget*: 75 miles/day
- *Forecast Horizon*: 4 days
- *Vulnerability Penalty*: 100 WFPI

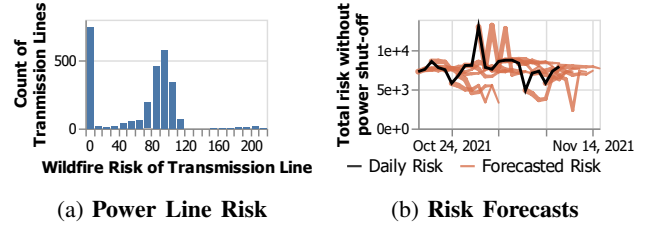


Fig. 1: **System Wildfire Risk Data**: 1a shows a histogram of the wildfire risk of individual transmission lines, based on all realized wildfire risk observed in the month of October. 1b shows the realized (black) and forecasted (orange) wildfire risk for the overall system, calculated as the sum of all wildfire risk values across all lines. Each forecast is represented with a line that covers the next 7 days.

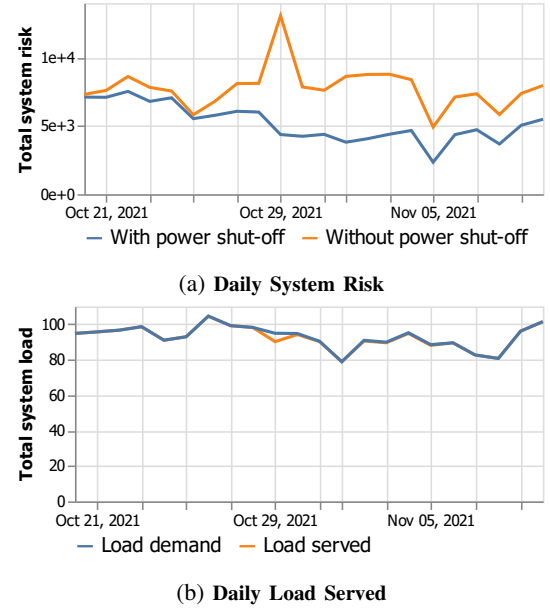


Fig. 2: Example MOPS problem. a) shows the reduction in risk as a result of turning off transmission lines. b) shows the reduction in load served, which primarily occurs on Oct 29th.

B. Baseline Solution

We first present the output of running this method in on the RTS-GMLC system using the baseline parameter settings. The MOPS problem is solved for each day, using information about the current status of the grid and the forecasted load and wildfire risk. The output is the shutoff and restoration actions, along with a DC power flow dispatch and load shed.

1) *Total system risk and load shed*: We first analyze the impact on total system risk and total load served for this baseline case. Fig. 2a shows the total system risk value without (orange) and with (blue) power shut-offs, and Fig. 2b shows the total load without (orange) and with (blue) power shut-offs. In the first few days of the case study, the grid risk is moderate. A small number of lines are de-energized to reduce the risk, but no load shed occurs. On Oct 29th, a large spike in risk occurs, leading to a significant grid shutoff, and resulting in around 5% load shed for this day. On Oct 30th, the wildfire risk values return to moderate levels,

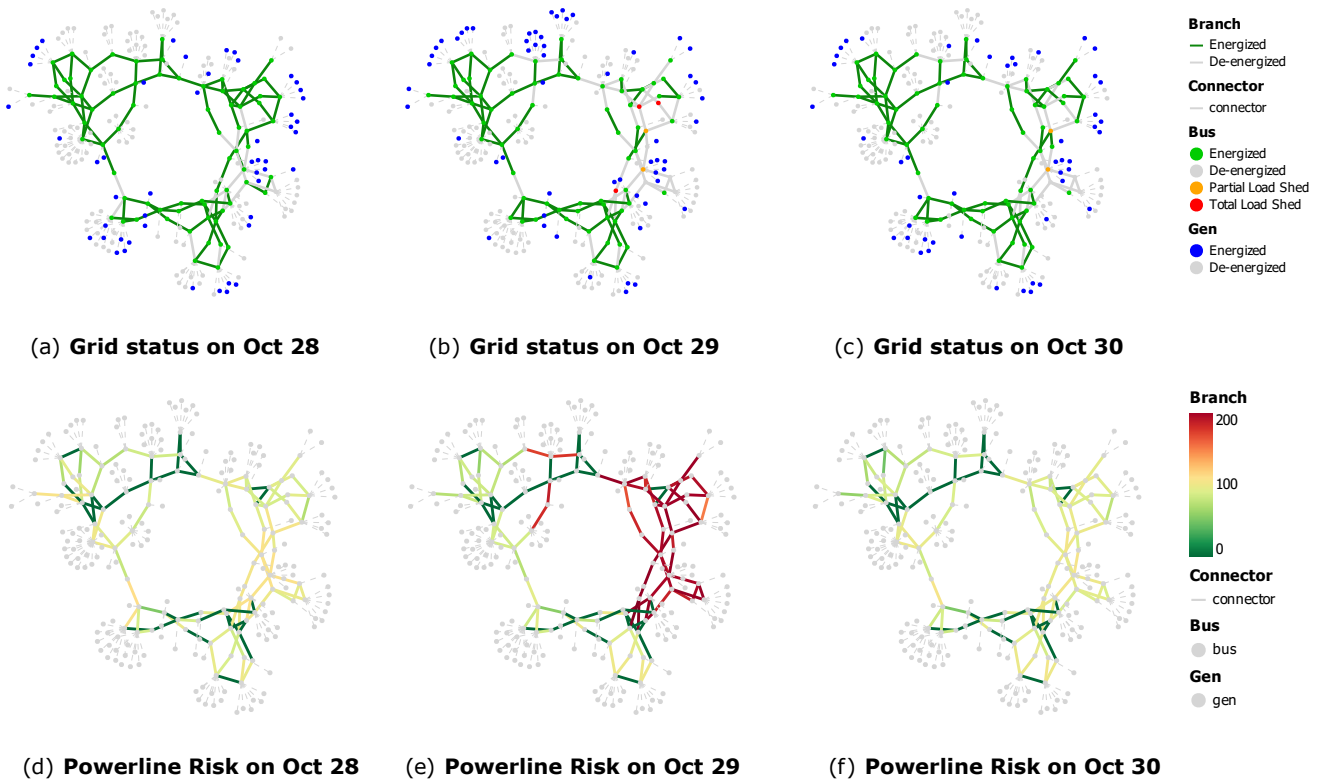


Fig. 3: **Power grid status and risk levels from Oct 28-30.** 3a-3c show the transmission lines status and 3d-3f show the transmission line risk values for Oct 28, 29 and 30. 3a October 28th shows a small power shutoff in response to the moderate risk, but no load shed. In 3b, A large spike in wildfire risk on Oct 29th prompted a large power shutoff in the eastern region on the grid leading to load shed at 5 nodes, 3 of which are fully shutdown. 3c shows the some recovery on Oct 30th as risk levels reduced. Sufficient lines have been repaired that only 2 nodes have partial load shed. In 3d shows the initial moderate risk levels on Oct 28th, where dark green lines are low risk and yellow lines are moderate risk. 3e shows a large spike in risk as much of the eastern region becomes high-risk red. The following day in 3f, risk levels return to moderate.

and sufficiently many lines are restored to avoid significant load shed. However, we observe that the total system risk after accounting for power shut-offs is lower than the total system risk without accounting for power shut-offs because many lines remain de-energized due to limited restoration resources.

2) *Geographical allocation of risk and load shed:* Next, we analyze how the load shed and wildfire risk is allocated geographically in the system. Figure 3 shows the state of the grid (top) and the wildfire risk values for each line (bottom) on Oct 28, 29 and 30. On Oct 28, there are several lines with risk values $R_{ijt} > V$ that are de-energized, but these de-energizations do not result in any load shed. On Oct 28, the wildfire risk has increased dramatically in the eastern region of the grid in 3e. This results in a large portion of the lines in this region to be turned off, as seen in 3b, but high risk lines remain energized to continue serving power. In total, there is partial load shed at 2 buses and total load shed at 3 buses. By Oct 30, the risk is reduced and many lines have been restored. There is still partial load shed at 2 buses, but no buses with total load shed.

3) *Solution times:* The baseline experiment involved solving the rolling horizon MOPS problem with a 4 day forecast

horizon for 21 days, and solved in 47 seconds. However, we note that the solve time is highly dependent on the problem parameters, in particular to the vulnerability penalty V and α . In some instances it could take more than 12 hours to solve the problem.

C. Sensitivity to Forecast Horizon

Next, we investigate the impact of the forecast horizon on the solution. The USGS provides a seven day WFPI risk forecast. We expect that a longer horizon may improve the decision making, but also increase the size of the optimization problem and associated solve time.

We first assess the impact on the objective function. We calculate the total load shed (1), total system risk (2) and system vulnerability (3) based on the final decisions and true realized wildfire risk and sum the values across the entire decision horizon. Table I(a) show the 3 elements of the objective function (after scaling by the factor α) and the final objective function value for forecast horizons from 1 to 7 days. Figure 4 shows the percentage of load served D_{Served}/D_{Tot} , the percentage of wildfire risk R_{Fire}/R_{Tot} and the normalized system vulnerability V_{System}/R_{Tot} .

From this I(a), we observe that the total objective function value improves by approximately 4.3% as the forecast

TABLE I: Results for different forecast horizons.

(a) Objective Value Metrics.							
Horizon (days)	1	2	3	4	5	6	7
Load Obj	0.297	0.298	0.299	0.299	0.299	0.299	0.299
Risk Obj	-0.380	-0.419	-0.456	-0.468	-0.493	-0.508	-0.507
Vulnerability Obj	-0.322	-0.275	-0.234	-0.222	-0.195	-0.179	-0.180
Total Obj	-0.404	-0.396	-0.391	-0.391	-0.389	-0.388	-0.387

(b) Line Energization and De-energization Events							
Horizon (days)	1	2	3	4	5	6	7
Lines Energized	61	58	61	59	57	55	57
Lines De-energized	93	85	84	84	80	76	75
Budget Used	1316	1330	1436	1336	1364	1286	1351

(c) Risk of Energized and De-energized Lines							
Horizon (days)	1	2	3	4	5	6	7
Energized Line Risk	Avg	50	52	54	55	56	57
	Min	0	0	0	0	0	0
	Max	198	208	206	206	208	208
De-energized Line Risk	Avg	100	102	104	105	106	107
	Min	1	1	17	8	40	40
	Max	215	215	215	215	215	215

horizon increases from 1 to 7 days, with the most significant improvements achieved within 3 days (3.3%). From Figure 4, we see that forecast horizon has a very small impact on the total load served. The major difference is that for shorter horizons, the total system risk is smaller, while the vulnerability penalty is higher. This implies that fewer lines are de-energized when a longer horizon is used, resulting in higher overall risk but a smaller vulnerability penalty. The reason behind this trend is that a shorter time horizon underestimates the vulnerability penalty because it does not consider future periods where a line is still disabled.

To support this argument, Table I(b) shows the total line energization and de-energization events that occur during the 21 day period. The forecast horizon has a major impact on the number of de-energized lines. We observe 93 de-energizations with a 1-day horizon, which is reduced to 75 de-energizations when using a 7-day horizon. Meanwhile, the number of line restorations is comparable in the two problems, with 61 restorations when using a 1-day horizon compared with 57 restorations when using a 7-day horizon. We conclude that the longer period problem disabled fewer devices because it considered the amount of time that devices would spend de-energized before they are repaired.

We see further evidence of this when considering the risk values of de-energized and energized lines. Table I(c) shows the average, maximum and minimum risk for the lines. Notably, both the average and minimum line risk for de-energized lines is smaller for shorter forecast horizons, indicating that more low-risk lines remain de-energized due to a lack of restoration budget. Finally, the forecast horizon has a significant impact on solve time, which increases from 10.35 s for the 1-day horizon to 46.98s for a 4-day horizon and to 296.33s for the 7-day horizon.

D. Sensitivity to Forecast Accuracy

As observed in Fig. 1b, there are substantial forecast errors associated with the wildfire risk forecast. To test

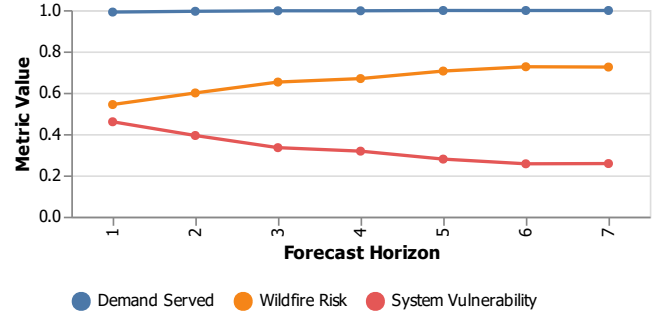


Fig. 4: Variation in objective function components for different forecast horizons.

TABLE II: Objective values obtained with perfect forecasts for different forecast horizons.

Horizon (days)	1	2	3	4	5	6	7
Load Obj	0.297	0.298	0.299	0.299	0.299	0.299	0.299
Risk Obj	-0.380	-0.419	-0.456	-0.468	-0.493	-0.508	-0.507
Vulnerability Obj	-0.322	-0.275	-0.234	-0.222	-0.195	-0.179	-0.180
Total Obj	-0.404	-0.396	-0.391	-0.391	-0.389	-0.388	-0.387

the impact of forecast errors on the results, we solve the same MOPS problem for forecast horizons varying from 1 to 7 days, but assume perfect information about the future wildfire risk (i.e., we use the realized risk data for each day rather than applying the risk forecast made for each day). Table II shows the resulting objective value metrics for each problem. When comparing these and other results to the solutions obtained with the forecasted data (discussed above in Table I), we observed that the solutions are more or less identical (although the solution time is slightly lower). Based on this surprising discovery, we conclude that the problem is insensitive to the forecast errors present in the wildfire risk data. This may be because shut-off decisions can be made instantaneously based on realized wildfire risk values, and restoration decisions can also be adapted after the true wildfire risk is known.

E. Sensitivity to Restoration Budget

The restoration budget Y_t determines how many miles of transmission lines can be restored each day. We solve the MOPS problem for each day in our 21 day horizon with different restoration budgets. Table III show the result of varying the restoration budget on the objection value (top), the number of de-energized and restored lines (middle) and the risk associated with energized and de-energized lines (bottom).

For the objective function value in Table III(a), we observe a similar trend as for increasing forecast horizon; the total objective value increases with a larger budget, but only by a few percent. However, a larger restoration budget implies a larger total system risk and smaller vulnerability penalty, as lines that were de-energized can be restored faster. When comparing the number of lines that are either de-energized or restored in Table III(b), we observe that a larger restoration budget significantly increases both the number of de-energized and restored lines. In particular, solution with a

TABLE III: Results for different restoration budgets.

(a) Objective Value Components.

Restoration Budget	25	50	75	100	125
Load Obj	0.299	0.299	0.299	0.299	0.299
Risk Obj	-0.436	-0.461	-0.468	-0.480	-0.488
Vulnerability Obj	-0.264	-0.233	-0.222	-0.207	-0.196
Total Obj	-0.402	-0.395	-0.391	-0.387	-0.385

(b) Line Energization and De-energization Events

Restoration Budget	25	50	75	100	125
Lines Energized	28	46	59	73	85
Lines De-energized	66	77	84	93	101
Budget Used	308	888	1336	1859	2344

(c) Risk of Energized and De-energized Lines

Restoration Budget	25	50	75	100	125
Energized Line Risk	Avg	54	55	55	55
	Min	0	0	0	0
	Max	208	208	206	206
De-energized Line Risk	Avg	100	103	105	106
	Min	1	8	8	40
	Max	215	215	215	215

small restoration budgets leaves a large number of lines de-energized at the end of the horizon. Furthermore, we observe in Table III(c) that the minimum transmission line risk for inactive lines increases as the budget increases. With a larger restoration budget, we can restore more de-energized lines with low risk quickly.

F. Sensitivity to Vulnerability Penalty

The vulnerability penalty V can be interpreted as a threshold for the wildfire risk value. If the wildfire risk $R_{ijt} < V$, we will pay a penalty in the objective function for de-energizing line ij at time t . Thus, the result of increasing the vulnerability penalty is to keep higher risk lines active. To assess the impact of the choice of V on the solution, we solve the MOPS problem for the 21 day period with three different values $V = \{75, 100, 125\}$.

The impact of the vulnerability penalty is on the objective function components is shown in Fig. 5 and Table IV(a). Increasing the vulnerability penalty increases the total system risk, but also lowers the de-energization cost. Again, varying the vulnerability penalty has no impact on load served. The final objective value improves by a few percent as the vulnerability penalty is increased.

A higher vulnerability penalty reduces the number of de-energized lines in the network as seen in Table IV(b). With $V = 125$, only 21 high-risk lines are being de-energized, and all lines are restored. Furthermore, the minimum risk of any de-energized line is 140, as seen in Table IV(c). Thus, we can conclude that the group of de-energized lines corresponds to the few lines with a very high risk in Figure 1a.

One major impact of increasing the vulnerability penalty is a decrease in the solve time of the problem. A vulnerability penalty of 75 results in a total solve time of 2,026 seconds, compared to 11 seconds when the vulnerability penalty is 125. A higher penalty limits the viable lines to de-energize, and allowing the mixed-integer solver to identify optimal solutions more quickly.

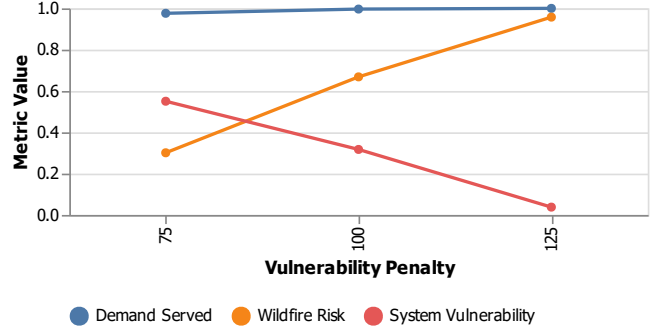


Fig. 5: Vulnerability Penalty Sensitivity: Bar plot of objective components when the vulnerability penalty changes

TABLE IV: Results for different vulnerability penalties.

(a) Objective Value Components.

Vulnerability Penalty	75	100	125
Load Obj	0.293	0.299	0.300
Risk Obj	-0.211	-0.468	-0.670
Vulnerability Obj	-0.514	-0.222	-0.021
Total Obj	-0.432	-0.391	-0.392

(b) Line Energization and De-energization Events

Vulnerability Penalty	75	100	125
Lines Energized	74	59	21
Lines De-energized	130	84	21
Budget Used	1398	1336	481

(c) Risk of Energized and De-energized Lines

Vulnerability Penalty	75	100	125
Energized Line Risk	Avg	37	55
	Min	0	0
	Max	206	206
De-energized Line Risk	Avg	95	105
	Min	1	8
	Max	215	215

IV. CONCLUSION

Wildfire threats to power grid infrastructure are increasing, and public safety power shutoffs (PSPS) represent an effective short-term method to reduce the risk of wildfire ignitions by the electric grid. However, PSPS are challenging to plan due to the time-varying nature of wildfire risk, as well as need to limit the size of power outages that may last for several days while utility crews work to restore power. To address this challenge, we propose a rolling horizon optimization problem, the Multi-period Optimal Power Shutoff (MOPS) problem, that co-optimizes decisions on where and when to de-energize power lines while also providing a schedule for how to restore them. The MOPS problem is implemented in a rolling horizon framework where the schedules are re-optimized on a daily basis as new information about wildfire risk become available.

We apply the proposed method to the RTS-GMLC system to analyze the performance as well as the sensitivity to the forecast horizon, restoration budget, and vulnerability penalty. We find that (1) a longer forecast horizon better accounts for the impact of de-energizing a line, (2) the

solution is insensitive to forecast errors related to the wildfire risk, (3) a larger restoration budget allows for disabling and restoring more lines, and (4) a higher vulnerability penalty incentivizes as solution where fewer lines are de-energized and they are restored more quickly.

The proposed framework has some limitations. The model uses a linear approximation of the power flow to accelerate the solution time, but this may lead to solutions that are not AC power flow feasible. In addition, despite the linear approximation, the problem can still be very slow to solve even on a small network. Heuristic solution techniques may be necessary to plan a PSPS on a realistic scale power network. In future work, we aim to develop algorithms that can solve MOPS in real-time for large systems during wildfire risk events and incorporate constraints that guarantee the resiliency and reliability of PSPS solutions to additional contingency events. We hope to eventually solve an AC-feasible MOPS problem with N-1 security constraints for a synthetic version of the California grid.

V. ACKNOWLEDGMENTS

The authors would like to acknowledge Sofia Taylor for helping obtain wildfire risk data for the RTS-GMLC system.

REFERENCES

- [1] V. B. R. Commission, Ed., *Final report*. Melbourne: Parliament of Victoria, 2009 Victorian Bushfires Royal Commission, 2010.
- [2] "Stats & Events." [Online]. Available: <https://www.fire.ca.gov/stats-events/>
- [3] D. N. Trakas and N. D. Hatzigiorgiou, "Optimal distribution system operation for enhancing resilience against wildfires," *IEEE Trans. on Power Systems*, vol. 33, no. 2, pp. 2260–2271, 2018.
- [4] M. Choobineh, B. Ansari, and S. Mohagheghi, "Vulnerability assessment of the power grid against progressing wildfires," *Fire Safety Journal*, vol. 73, pp. 20–28, 2015.
- [5] S. Dian, P. Cheng, Q. Ye, J. Wu, R. Luo, C. Wang, D. Hui, N. Zhou, D. Zou, Q. Yu, and X. Gong, "Integrating wildfires propagation prediction into early warning of electrical transmission line outages," *IEEE Access*, vol. 7, pp. 27 586–27 603, 2019.
- [6] S. Jazebi, F. de León, and A. Nelson, "Review of wildfire management techniques—part i: Causes, prevention, detection, suppression, and data analytics," *IEEE Trans. on Power Delivery*, vol. 35, no. 1, pp. 430–439, 2020.
- [7] —, "Review of wildfire management techniques—part ii: Urgent call for investment in research and development of preventative solutions," *IEEE Trans. on Power Delivery*, vol. 35, no. 1, pp. 440–450, 2020.
- [8] A. Arab, A. Khodaei, R. Eskandarpour, M. P. Thompson, and Y. Wei, "Three lines of defense for wildfire risk management in electric power grids: A review," *IEEE Access*, 2021.
- [9] J. W. Muhs, M. Parvania, and M. Shahidehpour, "Wildfire risk mitigation: A paradigm shift in power systems planning and operation," *IEEE Open Access Journal of Power and Energy*, vol. 7, pp. 366–375, 2020.
- [10] "PG&E Announces Major New Electric Infrastructure Safety Initiative to Protect Communities From Wildfire Threat | PG&E." [Online]. Available: <https://tinyurl.com/5bzkyt6d>
- [11] "PSPS Update: Power Restored for Essentially All Affected Customers After Dry, Offshore Wind Event and Exceptional Drought Conditions Prompt Safety Shutoff | PG&E." [Online]. Available: <https://tinyurl.com/2v8ajfum>
- [12] "Utility Company PSPS Post Event Reports." [Online]. Available: <https://www.cpuc.ca.gov/consumer-support/psps/utility-company-psps-post-event-reports>
- [13] N. Rhodes, L. Ntamo, and L. Roald, "Balancing wildfire risk and power outages through optimized power shut-offs," *IEEE Trans. on Power Systems*, vol. 36, no. 4, pp. 3118–3128, 2020.
- [14] W. Hong, B. Wang, M. Yao, D. Callaway, L. Dale, and C. Huang, "Data-driven power system optimal decision making strategy under-wildfire events," Lawrence Livermore National Lab.(LLNL), Livermore, CA (United States), Tech. Rep., 2022.
- [15] A. Ummakwe, M. Parvania, H. Nguyen, J. D. Horel, and K. R. Davis, "Data-driven spatio-temporal analysis of wildfire risk to power systems operation," 2020.
- [16] A. Lesage-Landry, F. Pellerin, J. A. Taylor, and D. S. Callaway, "Optimally scheduling public safety power shutoffs," *arXiv preprint arXiv:2203.02861*, 2022.
- [17] A. Kody, R. Piansky, and D. K. Molzahn, "Optimizing transmission infrastructure investments to support line de-energization for mitigating wildfire ignition risk," *arXiv preprint arXiv:2203.10176*, 2022.
- [18] S. Kancherla and I. Dobson, "Heavy-tailed transmission line restoration times observed in utility data," *IEEE Trans. on Power Systems*, vol. 33, no. 1, pp. 1145–1147, 2018.
- [19] N. Rhodes, D. M. Fobes, C. Coffrin, and L. Roald, "Powermodelsrestoration.jl: An open-source framework for exploring power network restoration algorithms," *Electric Power Systems Research*, vol. 190, p. 106736, 2021.
- [20] "Wildland fire potential index (wfpi)." [Online]. Available: <https://www.usgs.gov/fire-danger-forecast/wildland-fire-potential-index-wfpi>
- [21] B. Kocuk, H. Jeon, S. S. Dey, J. Linderoth, J. Luedtke, and X. A. Sun, "A cycle-based formulation and valid inequalities for dc power transmission problems with switching," vol. 64, no. 4, 2016. [Online]. Available: <https://doi-org.ezproxy.library.wisc.edu/10.1287/opre.2015.1471>
- [22] J. Bezanson, A. Edelman, S. Karpinski, and V. Shah, "Julia: A fresh approach to numerical computing," *SIAM Review*, vol. 59, no. 1, pp. 65–98, 2017. [Online]. Available: <https://doi.org/10.1137/141000671>
- [23] Gurobi Optimization, Inc., "Gurobi optimizer reference manual," Published online at <http://www.gurobi.com>, 2014.
- [24] C. Barrows, A. Bloom, A. Ehlen, J. Ikäheimo, J. Jorgenson, D. Krishnamurthy, J. Lau, B. McBenett, M. O'Connell, E. Preston, A. Staid, G. Stephen, and J.-P. Watson, "The iee reliability test system: A proposed 2019 update," *IEEE Trans. on Power Systems*, vol. 35, no. 1, pp. 119–127, 2020.
- [25] PGLib Optimal Power Flow Benchmarks, "The iee pes task force on benchmarks for validation of emerging power system algorithms," Published online at <https://github.com/power-grid-lib/pglib-opf>, 2021.
- [26] S. Taylor and L. A. Roald, "A framework for risk assessment and optimal line upgrade selection to mitigate wildfire risk," *arXiv preprint arXiv:2110.07348*, 2021.